

RESEARCH ARTICLE | FEBRUARY 16 2024

# On the modification of tip leakage noise sources by over-tip liners

Sergi Palleja-Cabre   ; Ivan Saraceno  ; Paruchuri Chaitanya 



*Physics of Fluids* 36, 026114 (2024)

<https://doi.org/10.1063/5.0187951>



CrossMark



**Physics of Fluids**  
Special Topic:  
Flow and Civil Structures

**Submit Today**



# On the modification of tip leakage noise sources by over-tip liners

Cite as: Phys. Fluids **36**, 026114 (2024); doi: [10.1063/5.0187951](https://doi.org/10.1063/5.0187951)  
Submitted: 17 November 2023 · Accepted: 22 January 2024 ·  
Published Online: 16 February 2024



View Online



Export Citation



CrossMark

Sergi Palleja-Cabre,<sup>a)</sup>  Ivan Saraceno,<sup>b)</sup>  and Paruchuri Chaitanya<sup>c)</sup> 

## AFFILIATIONS

Institute of Sound and Vibration Research, University of Southampton, Southampton, United Kingdom

<sup>a)</sup> Author to whom correspondence should be addressed: [spc1e17@soton.ac.uk](mailto:spc1e17@soton.ac.uk)

<sup>b)</sup> Electronic mail: [is1e20@soton.ac.uk](mailto:is1e20@soton.ac.uk)

<sup>c)</sup> Electronic mail: [ccp1m17@soton.ac.uk](mailto:ccp1m17@soton.ac.uk)

## ABSTRACT

Over-Tip-Rotor (OTR) liners have been investigated over the last decades as a technology to further reduce fan broadband noise in turbofan engines. The suppression of noise with OTR liners is attributed to conventional attenuation of acoustic waves and source modification effects. This paper describes a fundamental experiment to gain a better understanding of the source modification effects and establish whether they are purely due to acoustic back-reactions or also due to hydrodynamic changes on the source. The OTR liner configuration is approximated by a static airfoil with its tip located over a flat plate containing a flush-mounted liner insert and separated from the airfoil tip by a small gap. Synchronous measurements of the far-field noise and wall pressure fluctuations on the airfoil tip have shown that the reduction of wall pressure at the airfoil tip by the liner is the dominant mechanism of noise reduction. The reduction in unsteady pressure fluctuations on the airfoil tip by the liner is mainly caused by back-reaction effects at high frequencies and hydrodynamic modifications at low- and mid-frequencies. Over-tip liners are found to alter the unsteady flow field in the gap region and weaken the flow structures responsible for the generation of tip noise. This study has shown that far-field noise predictions based on analytical models are useful to estimate the performance of over-tip liners, but a complete assessment should also include the impact of the liner on the tip-leakage flow, and, consequently, the sources of tip noise.

© 2024 Author(s). All article content, except where otherwise noted, is licensed under a Creative Commons Attribution (CC BY) license (<http://creativecommons.org/licenses/by/4.0/>). <https://doi.org/10.1063/5.0187951>

## I. INTRODUCTION

Fan broadband noise is predicted to become an increasingly dominant source at takeoff in the next generation of commercial UltraHigh By-pass-Ratio (UHBR) engines.<sup>1</sup> Acoustic liners are widely used in industry to attenuate noise and are conventionally installed in the intake and bypass ducts of modern commercial aircraft engines. Maximizing the treated area is always a key parameter in liner performance. Over-Tip-Rotor (OTR) acoustic treatments have been investigated during the last decade as a technology with the potential to increase the treated area and further suppress fan noise.<sup>2–5</sup> The benefits of OTR liners can be especially relevant for new turbofan designs with shorter nacelles and compact ducted fans used in some propulsion architectures of Urban Air Mobility (UAM) vehicles.

Published experimental work<sup>2–5</sup> has attributed the noise reductions of OTR liners mainly to a combination of conventional attenuation of acoustic waves propagating over the liner and to a modification of the source itself. Analytical models to predict the noise suppression of OTR liners in cylindrical ducts<sup>6,7</sup> have shown that the Sound Power

Level Insertion Loss (PWL IL) of OTR liners can be divided into two contributions: (1) the noise attenuation, equivalent to the Transmission Loss (TL), and (2) the source modification due to acoustic back-reaction effects on the source for the lined and hard wall (HW) cases. The second contribution is related to a different source power output when a point source is located close to a hard wall or lined wall. The analytical models indicate that the source sound power decreases as the source approaches a suitably designed lined wall. This is in contrast to the behavior of a hard wall, in which the power output gradually increases with the proximity to the wall and is bounded to twice the free-field source power.

Over-Tip-Rotor liners were also experimentally studied<sup>8</sup> by using a simplified setup inspired by the work of Grilliat *et al.*<sup>9</sup> and Jacob *et al.*<sup>10</sup> The fan rotor and OTR liner were represented by a static airfoil with its tip located over a flat plate. The flat plate could be rigid or contain a flush-mounted liner insert separated from the airfoil tip by a small gap. Despite the simplifications of this setup, it captures key mechanisms of tip leakage noise<sup>10</sup> and is therefore useful for the

investigation of over-tip liners. The terminology “over-tip liner” is used in the current manuscript to refer to the OTR treatment in studies employing a static airfoil. The study<sup>8</sup> showed that the noise reduction benefits of the over-tip liner are reduced when increasing the gap size. This result agreed with an analytical prediction model based on a discrete evaluation of Thomasson formulation<sup>11</sup> for a monopole point source located over an infinite lined plane. The results were inconclusive, however, in determining the balance between the noise attenuation and the source modification effects.

This problem was also recently studied analytically by Sun *et al.*<sup>12</sup> by using a coupled singularity method. It was found that the OTR liners can alleviate the unsteady blade loading and that the close proximity to the fan intensifies the fluid particle oscillation through the acoustically treated wall and the sound dissipation. The predicted alleviation of the unsteady blade loading is in agreement with the experimental results previously presented in a preliminary version of the current work.<sup>13</sup> A recent computational study<sup>14</sup> has also shown that the enhanced particle velocity at the over-tip liner facing sheet, strongest at the resonance frequency of the liner, acts as a secondary source in anti-phase with the primary tip leakage noise sources. The interference between the primary and secondary noise sources also referred to as the back-reaction effect was identified as the key mechanism of the acoustic source modification in the absence of flow.

Previous work has solely considered linear acoustic effects to explain the enhanced noise reduction performance of OTR liners, including the back-reaction effects on the source explained above. The potential impact of the liner in affecting the unsteady flow field on the blade tip region and the related generation of tip-leakage noise has, however, not been addressed. A recent numerical investigation<sup>15</sup> has shown that the orifice flow in an OTR liner installed over a ducted fan can interact with the blade tip leakage flow and affect the development of the tip leakage vortex. This recent finding is additional evidence that over-tip liners might not only reduce noise through acoustic mechanisms but also by modifying the tip leakage flow. A summary of the different mechanisms of noise reduction in OTR liners proposed in the literature is shown in Fig. 1. These are (1) the conventional acoustic attenuation or sound absorption, and enhanced noise dissipation by the liner in close proximity to the tip sources, (2) the acoustic back-reaction effects on the source, and (3) the modified unsteady flow field in the tip region and related tip leakage noise.

The current investigation is focused on establishing more clearly the mechanisms of noise reduction of over-tip liners attributed to

source modification effects, that is the balance and significance of *acoustic* and *hydrodynamic* source modifications, (2) and (3), respectively, in Fig. 1. The static airfoil configuration used in previous work on over-tip liners<sup>8</sup> is adopted here by using a new setup in which tip-leakage noise is the dominant noise source and the airfoil is instrumented with pressure tapings on the tip region. Far-field and wall pressure measurements and hot-wire measurements in the tip region have been performed to investigate the impact of the liner on reducing tip leakage noise and on the flow field in the tip region. It will be experimentally shown, for the first time in the literature, that over-tip liners can modify the dominant sources of tip leakage noise both through acoustic back-reaction effects and mitigation of unsteady flow structures responsible for the generation of noise. In particular, the key findings of this work are

- Over-tip liners modify the unsteady wall pressure on the airfoil tip at locations relevant to the generation of tip-leakage noise.
- Over-tip liners are found to modify the sources of high-frequency tip leakage noise mainly through *acoustic* back-reaction effects on the source.
- Over-tip liners also weaken the coherent flow structures in the tip area responsible for the generation of tip leakage noise at low frequencies, hence providing a *hydrodynamic* source modification effect.

## II. DESCRIPTION OF THE EXPERIMENT

### A. Wind-tunnel and rig setup

The experiments were carried out at the Institute of Sound and Vibration Research’s open-jet wind tunnel facility. The wind tunnel is located within the anechoic chamber, of dimension  $8 \times 8 \times 8 \text{ m}^3$ . A nozzle of  $150 \times 450 \text{ mm}^2$  was used with a contraction ratio of 25:1 which provides a maximum flow speed of 100 m/s. A detailed description of the wind tunnel and its characteristics is provided in the literature.<sup>16</sup> The setup is shown in Fig. 2. It consists of an upper plate and a bottom plate mounted on the nozzle exit. The upper plate contains a rotating disk to hold the airfoil vertically and to change the angle of attack. The airfoil can slide into the upper plate to adjust the gap between the tip of the airfoil and the bottom plate. The bottom plate is either completely rigid or contains a flush-mounted liner insert over the tip of the airfoil. The maximum extent of the liner insert is  $300 \times 300 \text{ mm}$ , and it is indicated by the green area in Fig. 2(a). The liner configuration shown in Fig. 2(a), however, only covers the area

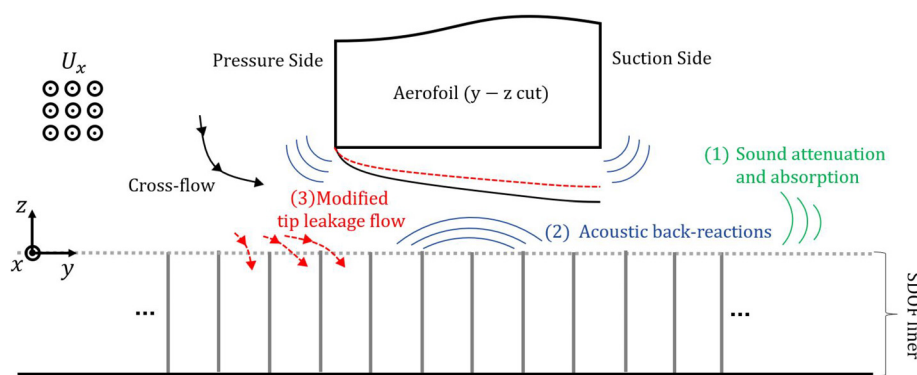


**FIG. 1.** Schematic of the proposed noise reduction mechanisms of over-tip liners: (1) acoustic attenuation and enhanced noise dissipation, (2) acoustic back-reaction effects on the source, and (3) modified unsteady flow field in the tip region and related tip leakage noise.

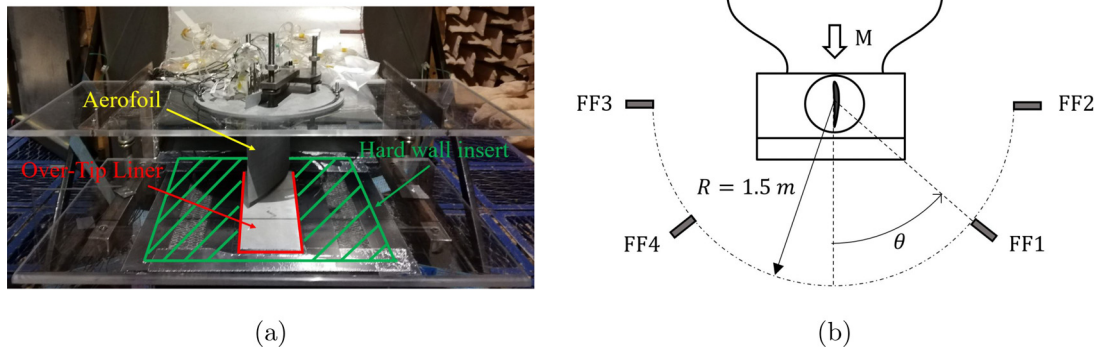


FIG. 2. Test setup for tip leakage noise: (a) photograph with the total insert area (green) and over-tip liner (red), and (b) sketch of the setup and far-field microphones.

immediately over the tip of the airfoil. The airfoil used in this study is a NACA5510 with a chord of 200 mm and a span of 150 mm. This cambered airfoil profile has been used in previous experimental<sup>9,10</sup> and computational<sup>17</sup> work on tip-leakage noise. The current experiments were performed for geometric angles of attack  $\text{AoA} = 10^\circ, 15^\circ,$  and  $20^\circ$  and flow speeds of  $U = 20, 30,$  and  $40$  m/s. The results in this manuscript are, however, presented only for  $\text{AoA} = 15^\circ$  and  $U = 40$  m/s.

**B. Over-tip liners**

Single-Degree-Of-Freedom (SDOF) cavity liners were used for this study. All liners were manufactured by following the procedure described in Ref. 8. A smooth aluminum wire mesh was bonded into a honeycomb structure with cavity depth  $h$ . Three different cavity depths were considered in this study:  $h = 20, 40,$  and  $60$  mm. The liners are therefore expected to present a linear behavior and to have minimal impact on the aerodynamic flow features. A liner sample was tested using an HBK BN-0293 portable impedance meter system type 9737.<sup>18</sup> Curve fitting of the impedance data to equation<sup>19</sup>

$$Z = R + j[M_r k - \cot(kh)], \tag{1}$$

where  $k$  is the wavenumber, yields a specific acoustic resistance  $R = 1.2$  and mass reactance  $M_r = 1.2$  mm. The results will be shown for a hard wall baseline [Fig. 3(a)] and an “over-tip” liner covering the area immediately over the tip of the airfoil [Fig. 3(b)].

It was shown by the authors<sup>13</sup> that the “over-tip” liner configuration immediately below the airfoil tip [Fig. 3(b)] of  $100 \times 300$  mm was

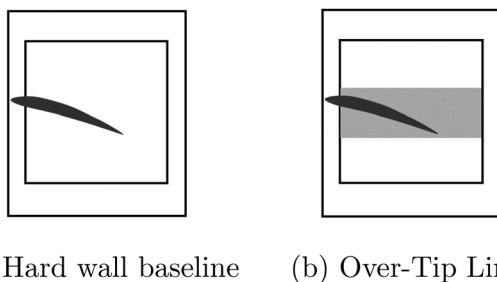


FIG. 3. Liner cases; blank areas represent a hard wall and meshed areas a lined surface.

sufficient to yield the same source modification effects, in terms of the wall pressures on the airfoil tip area, that a larger “full liner” configuration covering all the available square area of  $300 \times 300$  mm. Since the current investigation is targeted at gaining a better understanding of the source modification effects, results are presented only for the “over-tip” liner configuration.

**C. Far-field microphones, wall pressure probes, and flow measurements**

Far-field noise measurements were performed by using 4, 1/2 in. condenser microphones (B&K type 4189) located in the mid-span plane of the airfoil and at a constant radial distance of 1.5 m from the airfoil mid-chord position. Two microphones were placed on the suction side of the airfoil and two on the pressure side, each one at polar angles  $\theta = \pm 90^\circ$  and  $\theta = \pm 40^\circ$  relative to the downstream jet axis. Pressure measurements on the surface of the airfoil were also performed. The airfoil was instrumented with pressure taps in the tip region in the locations specified in Table I and shown in the sketch of Fig. 4(a); these are three positions along the chord at  $X/c = [0.25, 0.50, 0.75]$  on the airfoil bottom tip surface, indicated by green dots in Fig. 4(a), and at 1 mm from the tip on both the pressure and suction sides at  $X/c = [0.12, 0.25, 0.50, 0.75, 0.90]$ , indicated by red dots in Fig. 4(a).  $(X, Y, Z)$  is the airfoil-bound coordinates system, where  $X$  is aligned with the chord,  $Z$  with the span,  $Y$  is normal to the first two, and the origin is located on the tip leading edge of the airfoil. The pressure tappings on the airfoil surface and the over-tip liner are indicated in the close-up picture of the instrumented airfoil tip shown in Fig. 4(b). The pressure tappings were connected to remote electret condenser microphones (FG-23329-P07) with 0.75 mm diaphragm size. Far-field and wall pressure measurements were carried out simultaneously for a duration of 10 s at a sampling frequency of 40 kHz. The steady pressure at the pressure tapping positions was also measured separately for the different flow speeds, tip gaps, and liner configurations.

TABLE I. Locations of the surface pressure probes at the Tip and Pressure side (PS).

X (mm)	50	100	150	24	50	100	150	180	24	50	100	150	180
Z (mm)	0	0	0	1	1	1	1	1	1	1	1	1	1
Surface	Tip	Tip	Tip	PS	PS	PS	PS	PS	PS	PS	PS	PS	PS

04 March 2024 13:44:35

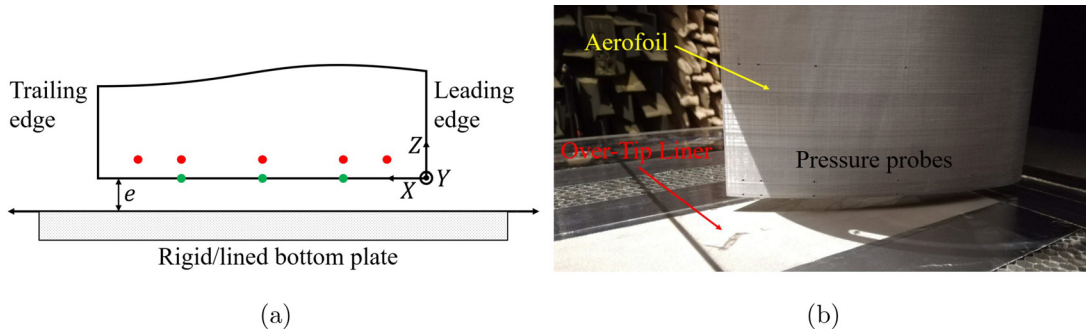


FIG. 4. Surface pressure probes: (a) sketch of the probe locations and (b) detail of the airfoil tip with the over-tip liner.

A hot-wire anemometer (TSI IFA-300 CTA, constant temperature anemometer) was used for measuring the velocity in the tip leakage region to understand the impact of an over-tip liner on the flow characteristics. The measurements were acquired synchronously with the far-field and the wall pressure probes for a duration of 6 s at a sampling frequency of 40 kHz. Three different hot-wire test matrices were considered for the hard and lined wall (“over-tip”) configurations with  $AoA = 15^\circ$  and  $U = 40$  m/s, which are outlined below. A global coordinate system  $(x, y, z)$  is now used where  $x$  is aligned with the inflow,  $z$  again with the airfoil span, and  $y$  is normal to the first two. The origin is now located on the bottom plate and indicated in Fig. 5.

- A single hot-wire probe was horizontally oriented and traversed along the suction side of the airfoil from a direction normal to the flow and at different heights from the hard/lined bottom plate [Fig. 5(a), red dots]. Hence, the probe was sensitive to velocity components contained in the  $y$ - $z$  plane. The extent of the traversed region is defined from 30% to 95% of the airfoil chord and vertically from  $z = 1$  mm from the bottom plate to a height of  $z = 15$  mm, with the airfoil tip located at  $z = 10$  mm.
- A hot-wire probe was also traversed over a plane normal to the hard/lined surface also horizontally oriented but from a direction parallel to the flow direction ( $x$  axis). That is, the probe was sensitive to velocity components contained in the  $x$ - $z$  plane. These

measurements were performed within the tip area, at a height of  $z = 5$  mm from the bottom plate [Fig. 5(a), blue dots], again with the airfoil tip located at  $z = 10$  mm.

- Two liner cells located immediately below the liner tip pressure side edge at 50% and 75% of the chord were instrumented with a hot wire probe. This was to assess any changes in the flow within the liner cavity cells induced by the three-dimensional tip leakage flow, which was found to have a significant vertical velocity component in these locations in previous stereo particle image velocimetry (PIV) tests performed on this setup.<sup>20</sup> In the current investigation, the hot-wire probe was located at the center of the honeycomb cells and at various depths  $d = 5$ – $15$  mm from the wire mesh plane (for a total cavity depth of  $h = 20$  mm), as indicated in Fig. 5(b). The instrumentation hole was sealed for each measurement to avoid leakage of flow from the test section. Two tip gaps of  $e = 5$  and  $10$  mm were considered in this instance.

### III. PREDICTED NOISE REDUCTION OF OVER-TIP LINERS

The performance of acoustic liners is often assessed by using the normal incidence absorption coefficient,  $\alpha$ , which for an SDOF cavity liner governed by Eq. (1) can be written as

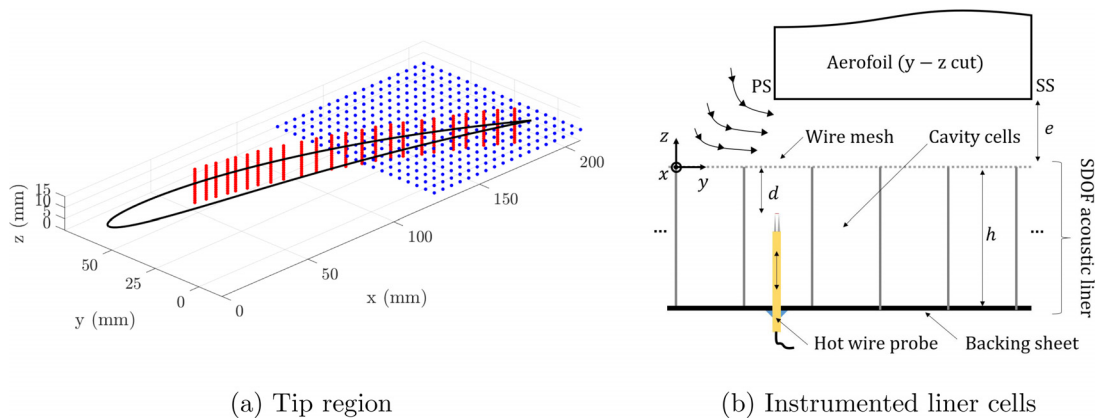


FIG. 5. Hot-wire measurements locations. In (a), the airfoil tip ( $e = 10$  mm) is indicated with the solid black line and the measurement locations with dots.



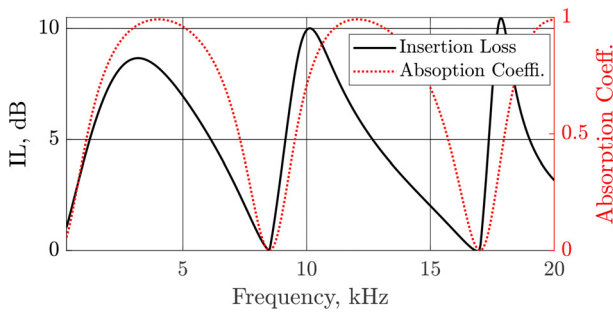


FIG. 6. Predicted PWL IL for a monopole source at  $e = 5$  mm and normal incidence absorption coefficient.

$$\alpha = \frac{4R}{(R + 1)^2 + [M_r k - \cot(kh)]^2}. \quad (2)$$

This is the approach used in previous experimental work for the design of OTR liners.<sup>5</sup> However, peak PWL Insertion Loss in OTR liner applications will often occur at different frequencies than the maximum absorption coefficient. This is because the latter does naturally not account for back-reaction effects on the source. This is shown in this section by comparing the predicted absorption coefficient with simplified analytical models for OTR liners. These models were compared with measured data of over-tip liners in previous work<sup>8</sup> and showed a good qualitative agreement. A physical interpretation of the back-reaction noise reduction mechanism will also be presented based on the coupling of the source strength and the particle velocity at the airfoil tip.

### A. Design of over-tip liners for maximum Insertion Loss

The predicted normal incidence absorption coefficient for the SDOF liner described in Sec. II B ( $h = 2$  cm) is shown in Fig. 6. The predicted PWL IL for the SDOF described in Sec. II B ( $h = 2$  cm) is obtained by using an analytical model of Levine.<sup>21</sup> It provides a closed-form analytical expression of the power radiation by a monopole source over an infinite lined plane. This is in the form of power amplification factors, defined as the ratio of the acoustic power radiated in

the presence of the plane ( $W$ ) to that radiated in free-field ( $W_f$ ). The power amplification factor corresponding to the power radiated away from the surface is expressed as

$$\frac{W}{W_f} = 1 + \frac{\sin z}{z} + 2\text{Re}\left(Ae^{iAz}\left[E_1(j[1+A]z) - E_1(jAz)\right]\right) - 2\text{Re}(A) \int_0^1 \frac{\mu d\mu}{|A + \sqrt{1 - \mu^2}|^2}, \quad (3)$$

where  $z = 2ke$ ,  $k$  is the wavenumber,  $e$  is the vertical distance from the point source to the liner surface, and  $E_1(\zeta)$  is defined as the integral

$$E_1(\zeta) = \int_{\zeta}^{\infty} \frac{e^{-\xi} d\xi}{\xi}, \quad |\arg(\zeta)| < \pi. \quad (4)$$

The predicted PWL IL obtained with Eq. (3) for a monopole source located at a vertical distance  $e = 5$  mm from the liner surface is also shown in Fig. 6. It is clear from these results that the peak IL occurs at frequencies significantly different from that of the absorption coefficient, and the difference gets more pronounced at the higher multiples of the resonance frequency. The frequencies corresponding to the maximum absorption coefficient simply require that the reactance  $X = M_r k - \cot(kh) = 0$ . Conversely, for a given facing sheet resistance  $R$  and tip gap  $e$ , the optimum reactance for maximum IL is dictated by the interference between the primary point source and the back reaction from the liner. This is illustrated in Fig. 7(a) by showing the resistance and reactance of the SDOF liner for different cavity depths,  $h$ , and the optimum reactance,  $X_{opt}$  indicated by the thick solid black line. The optimum reactance is obtained iteratively by evaluating Eq. (3) for the fixed resistance  $R$ , vertical distance  $e = 5$  mm, and a range of reactance  $X \in (-5, 5)$ . Peak IL is obtained at the frequencies where the liner reactance intersects the optimum reactance  $X_{opt}$ , indicated by the dots in Fig. 7(a). This simplified model, however, does not account for the finite length of the liner inserts, which would cause additional back-scattering effects from the impedance discontinuity at the liner terminations.<sup>14</sup>

The predicted PWL IL for a monopole source at  $e = 5$  mm for the three cavity depths tested in the current investigation is shown in Fig. 7(b). Also shown in Fig. 7(b) is the typical excess tip noise measured for the current configuration. This is obtained by subtracting the

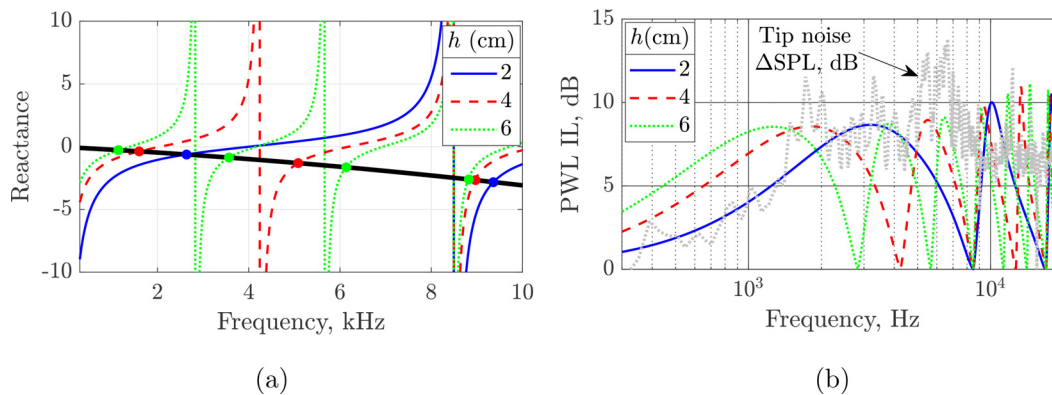


FIG. 7. Predicted (a) liner reactance and “optimum” reactance (thick black line), and (b) PWL IL for different cavity depths  $h$ . Also shown in (b) is the noise increase due to tip leakage (gray dotted line).

sound pressure level (SPL) in the far field ( $\theta = -90^\circ$ ) for the hard wall reference case without a tip gap ( $e = 0$  mm) from the case of a tip gap of  $e = 5$  mm. The current liner cavity depths were selected in order to yield peak PWL IL at frequencies where tip noise is dominant but also to obtain both peak IL and zero IL at similar frequencies. This is to investigate whether the noise reduction of over-tip liners is dominated by acoustic back-reaction effects or by hydrodynamic changes in the sources of tip leakage noise. If it is dominated by acoustic effects, the measured noise reduction should broadly follow the predictions from this section. Conversely, if hydrodynamic source modifications are dominant, the noise reductions are likely to be quite insensitive to the acoustic liner back-reaction effects. At the frequencies of anti-resonance ( $X \rightarrow \infty$ ), the liner behaves acoustically as a hard wall; therefore, both the absorption coefficient and the predicted IL are zero.

Predictions of the SPL Insertion Loss at the microphone locations of the measured data are shown later in Sec. IV. These are obtained by using a discrete evaluation of Thomasson formulation<sup>11</sup> for a monopole point source located over an infinite lined plane.<sup>8</sup> This approach accounts for a *dipole* source by considering two monopole sources of opposite phases separated by a distance  $\epsilon$  such that  $\epsilon \ll \lambda$  and  $\epsilon \ll e$  and was verified in the literature.<sup>8</sup> The predicted insertion loss, however, was shown to be very similar to the monopole source predictions shown earlier in this section.

### B. Interpretation of the back-reactions on the source

Tip leakage noise in the current setup has been associated with dipole noise sources.<sup>22</sup> A physical interpretation of the back-reaction noise reduction mechanism of over-tip liners is now presented. The sound power  $W$  at a single frequency  $\omega$  due to a point dipole source located at  $\mathbf{y}_s$  of the form

$$\mathbf{f}(\mathbf{y}, \omega) = \tilde{\mathbf{f}}(\omega)\delta(\mathbf{y} - \mathbf{y}_s), \quad (5)$$

where  $\tilde{\mathbf{f}}(\omega)$  is the complex dipole source strength and  $\delta(\mathbf{y})$  is the Dirac delta function, which is given by<sup>23,24</sup>

$$W = \frac{1}{2} \text{Re}\{\tilde{\mathbf{f}}(\omega) \cdot \tilde{\mathbf{u}}^*(\omega, \mathbf{y}_s)\}, \quad (6)$$

where “ $\cdot$ ” denotes the dot product, and  $\tilde{\mathbf{u}}^*(\omega, \mathbf{y}_s)$  is the complex conjugate of the acoustic particle velocity evaluated at the source location. In the current problem, the dipole strength is equal to the pressure jump across the blade tip

$$\tilde{\mathbf{f}}(\omega) = \Delta p(\omega)\mathbf{n}, \quad (7)$$

where  $\mathbf{n}$  is the unit vector normal to the blade tip. Interrogation of Eq. (6) suggests that the sound power generated at the blade tip is due to the coupling of the dipole source strength with the particle velocity at the tip location. There are therefore three methods for reducing the sound power radiated by the blade tip:

- (1) To reduce the variation in time of the pressure jump across the blade tip  $\Delta p(\omega)$ .
- (2) To reduce the particle velocity at the blade tip  $\tilde{\mathbf{u}}(\omega, \mathbf{y}_s)$ .
- (3) To ensure that the particle velocity is in quadrature (i.e.,  $\pi$  radians, out of phase) with the dipole source strength.

The most practical strategy is (3), which can be controlled by installing predominantly reactive acoustic liners at a short distance

from the blade tip. In the presence of the liner, the particle velocity has two contributions. The first is due to the dipole source itself  $\tilde{\mathbf{u}}_0(\omega, \mathbf{y}_s)$ . The second is due to the contribution from the liner  $\tilde{\mathbf{u}}_Z(\omega, \mathbf{y}_s)$ , i.e.,

$$\tilde{\mathbf{u}}(\omega, \mathbf{y}_s) = \tilde{\mathbf{u}}_0(\omega, \mathbf{y}_s) + \tilde{\mathbf{u}}_Z(\omega, \mathbf{y}_s). \quad (8)$$

Substitution of Eq. (8) into Eq. (6) suggests that the sound power from the blade tip in the presence of the liner is the sum of two contributions

$$W(\omega) = W_0(\omega) + W_Z(\omega), \quad (9)$$

where  $W_0(\omega)$  is again the sound power radiated by the tip source in the free field and  $W_Z(\omega)$  is the contribution in sound power due to the presence of the liner. This formulation is based on the same principles as the closed-form analytical expression of Eq. (3), although in that case for a monopole point source, but highlights explicitly the physics of the noise reduction mechanisms of over-tip liners. The interference between the primary point source and the secondary point source explained in the literature<sup>14</sup> as the mechanism of acoustic back-reaction effects is shown here to be equivalent to having the particle velocity and the dipole source strength out of phase.

Another way of reducing the power output of the tip leakage source would also be point (1) above; to reduce the pressure jump across the blade tip  $\Delta p(\omega)$ . Although the design of the over-tip liner to this end is not straightforward, it shall be shown later in the paper that the liner can modify the flow field in the tip region and, in turn, weaken the strength of the tip leakage noise source. Although this is clearly not an acoustic back-reaction effect on the source, but rather a hydrodynamic effect, its impact on the source power output is also captured in Eq. (6) by a reduction of  $\Delta p(\omega)$ .

## IV. RESULTS AND DISCUSSION

The results presented here are focused on a constant geometric angle of attack of  $\text{AoA} = 15^\circ$ , a flow speed of  $U = 40$  m/s, and a selection of far-field locations and pressure probes. The conclusions of this study are, however, also applicable to the other flow speeds and angles of attack tested in this investigation.

### A. Far-field acoustic measurements

The Sound Pressure Level (SPL) measured in the pressure side of the airfoil ( $\theta = -90^\circ$ ) for a hard wall configuration, a lined configuration [over-tip, Fig. 3(b),  $h = 20$  mm], and in grazing flow conditions is shown in Fig. 8(a). These are shown for the cases without a tip gap ( $e = 0$  mm, dashed lines) and with a tip gap of  $e = 10$  mm (solid lines). The grazing flow results (blue dotted line) were obtained without the airfoil in the test section and are regarded as background noise.

The tip leakage noise for the case of a hard wall casing is determined here by the direct subtraction of the SPL for the zero-gap baseline from the cases with a tip gap. In the current manuscript, the subtraction is performed directly at each far-field microphone location as

$$\Delta \text{SPL} \text{ (dB)} = 10 \log_{10}(S_{\text{pp, total}}) - 10 \log_{10}(S_{\text{pp, no gap}}), \quad (10)$$

where  $S_{\text{pp}}$  is the power spectral density of the far-field acoustic pressure. The resulting excess tip noise for the results in Fig. 8(a) is shown in Fig. 8(b). The sources of tip noise in such configuration have been studied experimentally<sup>10,25</sup> and numerically<sup>17</sup> in the literature. More

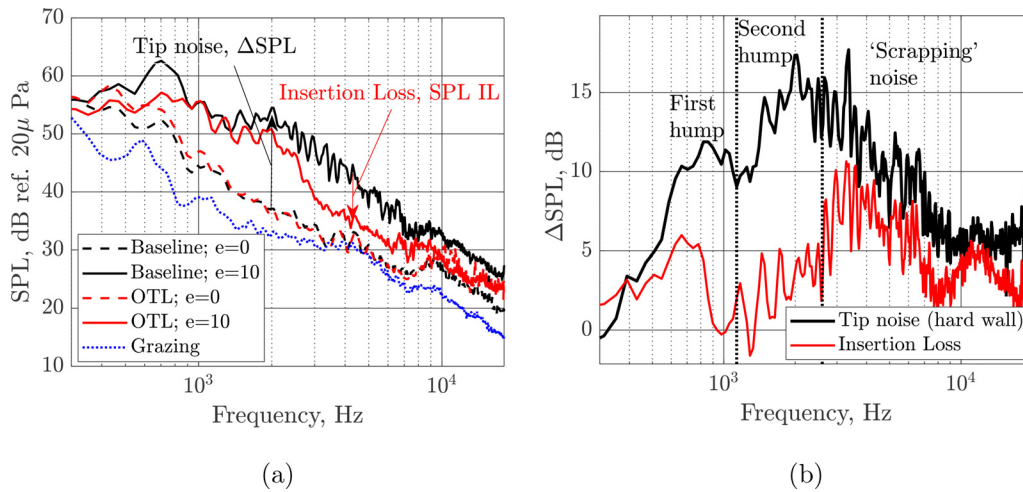


**FIG. 8.** Typical far-field characteristics of tip leakage noise: (a) SPL spectra for hard wall and lined (over-tip,  $h = 20$  mm) cases for  $e = 0$  mm and  $e = 10$  mm and (b) excess tip noise relative to  $e = 0$  mm and SPL Insertion Loss for  $e = 10$  mm.

recently, the sources of tip noise in the current setup have also been experimentally investigated by the authors of Refs. 20 and 22. The mean features are indicated in Fig. 8(b) and summarized below:

- **First hump:** the noise at frequencies around  $f = 800$  Hz was found to be related to shed vorticity from the shear layer caused by the flow separation at the pressure side tip edge.<sup>22</sup> This flow structure and the related first hump are not found, however, for a lower tip gap of  $e = 5$  mm, as shown by the dotted line in Fig. 7(b).
- **Second hump:** the second source of noise, here at frequencies between  $1100 < f < 1600$  Hz is attributed to the unsteady pressures on the airfoil surface induced by flow instabilities that produce smaller scale structures than the first hump.<sup>22</sup>
- **“Scrapping” noise:** the noise at frequencies above the second hump ( $f > 2600$  Hz for  $U = 40$  m/s) is attributed to “scrapping”<sup>17,26</sup> or interaction of smaller turbulent structures along the airfoil tip edge.

The noise reduction due to a liner insert, or Insertion Loss, is obtained by subtracting, in dB scale, the SPL for the lined case from that of the baseline hard wall configuration (for a given gap size  $e$ )

$$\text{SPL IL (dB)} = 10 \log_{10} \left( S_{pp}^H \right) - 10 \log_{10} \left( S_{pp}^L \right), \quad (11)$$

where the superscripts H and L denote hard wall and lined wall, respectively. The SPL IL for the results in Fig. 8(a) is also shown in Fig. 8(b). It can be observed that this liner configuration yields up to 5 dB of noise reductions at frequencies of the first hump, but it is especially effective at the higher frequencies in which the “scrapping” noise along the airfoil chord is dominant.

The measured and predicted noise reductions for the Over-tip liners with different cavity depths  $h = 20, 40,$  and  $60$  mm are shown in Fig. 9 for tip gaps of  $e = 5$  and  $10$  mm at  $\theta = -90^\circ$ . Also shown in Fig. 9 is the excess tip noise for the hard wall configuration for the two values of the tip gap. The frequencies characterized by the “first hump,” “second hump,” and “scrapping noise” are indicated with

numbers ①, ②, and ③, respectively, and delimited by the vertical dotted lines, as previously shown in Fig. 8(b). Focusing first on the hard wall excess tip noise data, it can be observed once again that the “first hump” is not present for the case of  $e = 5$  mm and that the second hump is also significantly reduced. This is in line with previous work<sup>22</sup> as explained earlier in the section.

In the case of the smaller tip gap of  $e = 5$  mm [Figs. 9(a), 9(c), and 9(e)], the measured data indicate that the liners are most effective in reducing noise at the higher frequency range ③. The dominant source of tip noise at these frequencies is the scattering of incoherent eddies along the airfoil tip edge, which seems to be strongly reduced by the over-tip liners. At some frequencies, the excess noise is, in fact, almost fully suppressed. That is, when the SPL Insertion Loss (red line) is of the same level as the excess tip noise  $\Delta\text{SPL}$  of the hard wall configuration (black line), which represents an upper limit of noise reduction since the liner is found to be most effective in reducing sources located in its close vicinity.<sup>8</sup> Conversely, the liner is found to only provide weak noise suppression at frequencies in ②, which is discussed later. The liners are also found to not reduce noise over frequencies in ①. This is expected since the first hump is not present for  $e = 5$  mm and tip noise is therefore minimal at these frequencies.

In the case of the larger tip gap of  $e = 10$  mm [Figs. 9(b), 9(d), and 9(f)], the measured data also indicate that the noise reductions are generally stronger at the higher frequency range ③. However, in this case, the liners are also found to be effective over the frequencies of the first hump ① and the second hump ②, yielding up to 5 dB Insertion Loss.

The predictions obtained with the simplified analytical model in Sec. III are included in Fig. 9 to estimate the frequencies of peak Insertion Loss for the different cavity depths and tip gaps purely based on acoustic back-reaction and absorption. Due to the simplification of tip leakage noise to a point source, the model is naturally not capable of accurately predicting the absolute levels of SPL Insertion Loss. However, the results in Fig. 9 indicate that the analytical model is capable of capturing the frequencies of the peaks and deeps (anti-resonance) of noise reduction in ③, which occur at different frequencies



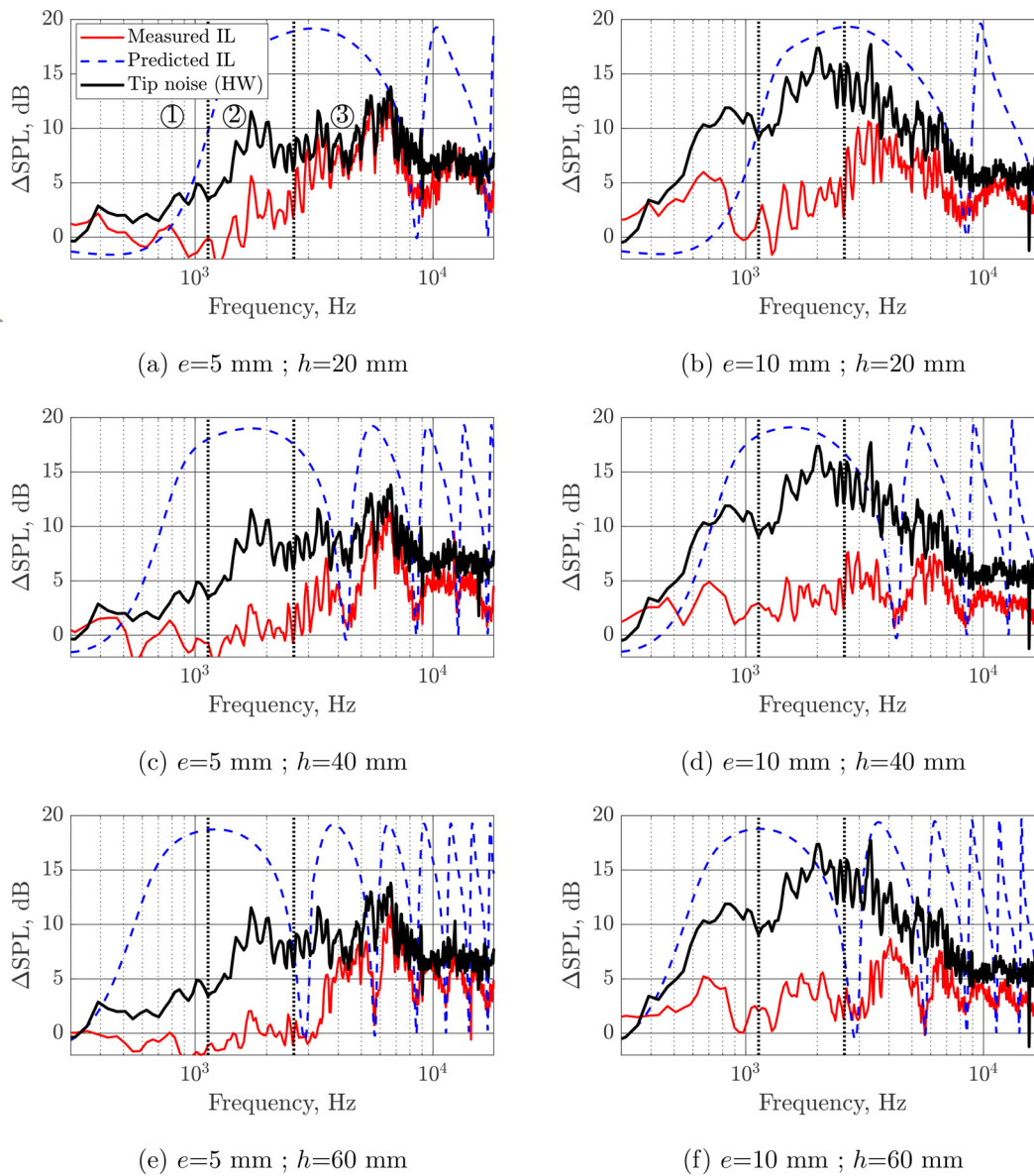


FIG. 9. Measured and predicted far-field SPL Insertion Loss and comparison to tip leakage excess noise of the hard wall (HW) configuration.

when varying the cavity depth  $h$ , indicating that the noise reduction at those frequencies is dominated by *acoustic* effects. Conversely, for the case with  $e = 10$  mm, the measured insertion loss over frequencies of the first and second humps ① and ② appears to be quite insensitive to the cavity depth, and in Fig. 9(b), it is in disagreement with the predicted insertion loss. This suggests that the noise reduction at these lower frequencies is likely not dominated by *acoustic* back-reaction effects but rather *hydrodynamic* changes on the source. It shall be shown later in Sec. IV C that the over-tip liners can modify the flow field and weaken these coherent flow structures, which is hypothesized as the main reason for the noise reduction over the range of

frequencies ① and ②. A weakened tip source also reduces the potential noise reductions of over-tip liners through *acoustic* back-reaction effects, which are also expected to contribute toward the measured insertion loss.

### B. Wall pressure fluctuations on the airfoil tip

The enhanced noise reduction of over-tip liners relative to conventional liners has been linked to source modification effects in the literature. These are caused by the close proximity of the tip sources to the liner surface, which has been found to cause *acoustic* back-reaction

effects on the source<sup>6,14</sup> and to alleviate the unsteady blade loading.<sup>12,13</sup> This section analyses the wall pressure fluctuations measured at different locations of the airfoil tip for the hard wall and over-tip liner configurations, which is shown experimentally here for the first time in the literature. The results in this section also aim to link the reductions in wall pressure fluctuations on the airfoil tip due to the over-tip liner to the reduction in far-field noise. The analysis presented here is based on a direct comparison of the noise reduction spectra measured on the airfoil tip and the far-field, and the drop in coherence between the two synchronous signals when an over-tip liner is considered.

Previous computational investigations<sup>17</sup> indicated that the dominant sources of tip-leakage noise with hard wall plates are located close to the mid-chord position. A recent experimental work<sup>22</sup> has explored further the tip-leakage noise mechanisms for the current setup and also highlighted the importance of the sources within 50% to 75% of the chord, linked to flow structures responsible for the first and second humps ① and ②. “Scraping” noise at the higher frequencies ③ has been hypothesized to be distributed along the tip edge where the cross-flow is stronger, in this case also around 50% of the chord. The results in this section are therefore focused on the two chordwise locations of 50% and 75% relevant for the noise sources and their suppression with over-tip liners. The results are presented here only for the pressure tapings on the pressure side tip of the airfoil since these were found to be the most affected by the over-tip liners. The wall pressures on the suction side and tip of the airfoil were found to be practically insensitive to the liner for the tip gaps studied in this investigation and are

therefore not included in this paper. The spectra of wall pressure at these two locations on the airfoil tip are shown in Fig. 10 for the hard wall and over-tip liner configurations (for different cavity depths  $h$ ) and for the tip gaps  $e = 5$  and 10 mm.

For the lower tip gap  $e = 5$  mm [Figs. 10(a) and 10(c)], the liners are found to reduce the wall pressures at the higher frequencies ③ by over 5 dB at both measurement locations. The effect of the liner is most pronounced at  $x/c = 0.50$  [Fig. 10(a)], where the cross-flow is stronger, with up to 12 dB of reduction. At this location, it is very clear that the peak reductions take place at different frequencies depending on the cavity depth  $h$ . The effect of the liner in modifying the wall pressures is, however, weaker at frequencies of ① and ② for this small tip gap. Conversely, for the larger tip gap  $e = 10$  mm, reductions over the whole spectra are observed at  $x/c = 0.50$  and  $x/c = 0.75$  [Figs. 10(b) and 10(d), respectively]. In the latter, reductions of up to 10 dB at frequencies of the first hump ① and 20 dB at the higher frequencies ③ can be observed. In addition, the frequencies of peak reduction in wall pressure at this measurement location ( $x/c = 0.75$ ) appear to be quite insensitive to the liner cavity depth  $h$ , which indicates that these are not caused by acoustic back-reaction effects on the source but rather hydrodynamic effects potentially related to changes in the tip flow structures.

The impact of the over-tip liners on the sources of tip leakage noise is investigated next by comparing the reduction in wall pressures and the insertion loss in the far-field in Fig. 11. The results are presented for the liner with the deepest cavities of  $h = 60$  mm. The

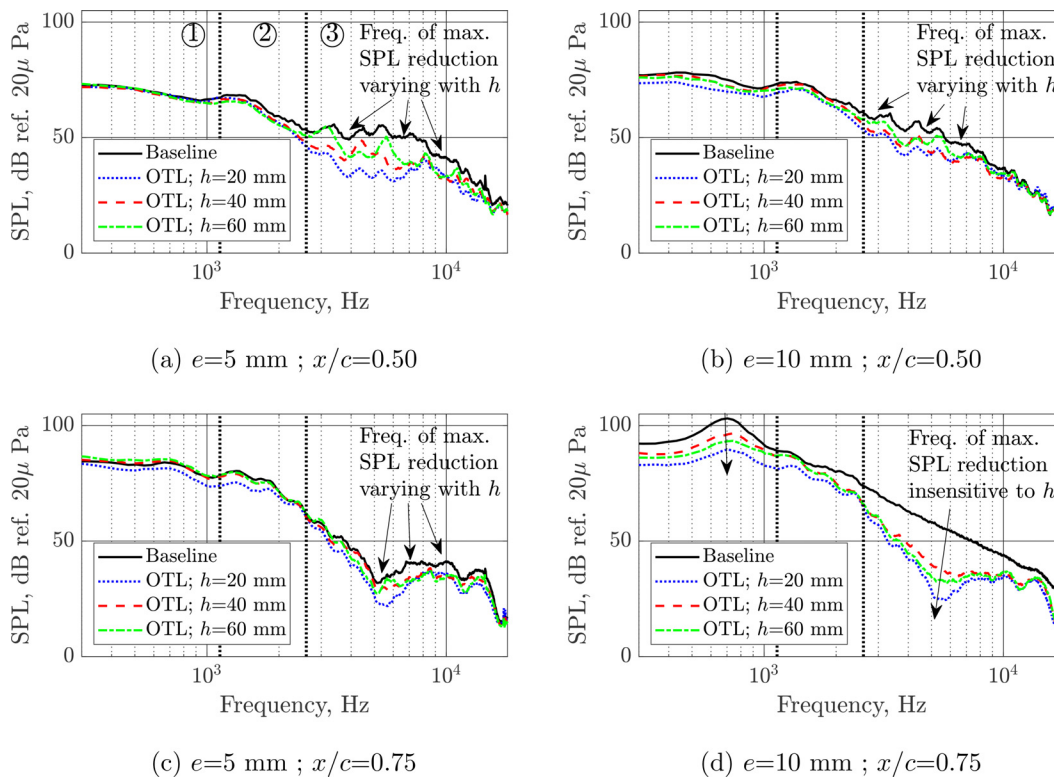


FIG. 10. Measured wall pressure fluctuations for the hard wall baseline and over-tip liners with different cavity depths  $h$ .

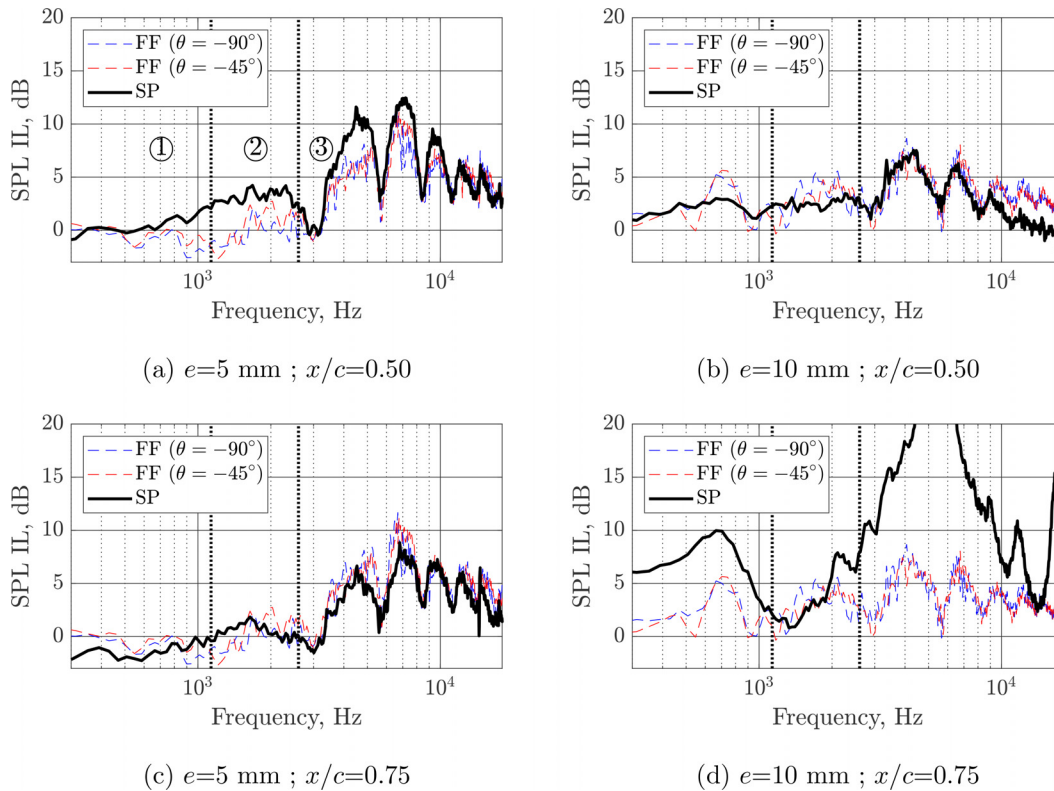


FIG. 11. Reduction in wall pressure (SP) and far-field (FF) SPL Insertion Loss on the pressure side tip for the over-tip liners with a cavity depth of  $h = 60$  cm.

reduction in wall pressures is shown by the thick solid black lines and the far-field insertion loss at two microphone locations on the pressure side with colored dashed lines. An excellent agreement both in magnitude and shape can be observed at both measurement locations along the chord for the lower tip gap  $e = 5$  mm [Figs. 11(a) and 11(c)]. For this tip gap, the peak noise reductions and the anti-resonances measured in the far-field can also be clearly seen as reductions in wall pressures, especially at the higher frequencies ③ where tip noise is strongest. This result supports the interpretation of the source modification effects as *acoustic* back-reactions on the source that effectively modify the power output of the tip source. In these circumstances, simple analytical models can provide guidance in the design of OTR liners for optimum noise reduction and tune them at target frequencies of interest.

The above observation, however, is less clear for the cases with the larger tip gap of  $e = 10$  mm [Figs. 11(b) and 11(d)] with a more complex flow topology related to the dominant sources of tip leakage noise. A good agreement between the reductions in wall pressure and far-field noise is found at  $x/c = 0.50$  [Fig. 11(b)], especially over the higher frequencies ③, but also with modest reductions over ① and ②. However, the reductions in wall pressures are much larger at  $x/c = 0.75$  [Fig. 11(d)]. It is clear that the over-tip liner induces a reduction of wall pressures at the frequencies of the first hump ①, which is also observed in the far-field. Reductions of over 20 dB are observed above these frequencies, especially in ③, which do not

present the peaks and deeps of noise reduction measured in the far-field and expected from the acoustic back-reaction effects. The spatially dependent behavior of the reductions in wall pressures, their link to the tip noise source generation mechanisms, and the lack of sensitivity to the liner depth for  $x/c = 0.75$  [Fig. 10(d)], all support the hypothesis that hydrodynamic changes on the source also play a significant role in the source modification effects of over-tip liners. These hydrodynamic changes mentioned above are hypothesized to be a combination of two different phenomena: (1) a weakening of the cross-flow and the related shear layer and unsteady flow features causing the sources of tip leakage noise, and (2) a displacement of the separated tip flow toward downstream chordwise locations. Point (1) will be discussed in greater detail in Sec. IV C. Point (2) is argued to be a key contributor to the large reductions in surface pressures at  $x/c = 0.75$  of over 20 dB observed in Fig. 10(d) and Fig. 11(d) when the liner is present since only 5 dB of noise reduction is measured in the far-field at those frequencies. In the over-tip liner case, the tip sources related to the cross-flow at those frequencies are likely located further downstream than  $x/c = 0.75$  but are still contributing to the far field noise, although weakened due to point (1).

The results in Fig. 11 are only shown for the case with  $h = 60$  mm because this is the case with a larger number of peak noise reductions and anti-resonances within the range of frequencies of interest. It therefore reflects more clearly the effects of acoustic back-reactions at higher frequencies, especially for  $e = 5$  mm, and highlights potential

hydrodynamic source modification effects for  $e = 10$  mm. The same conclusions are, however, also true for the cases with other cavity depths not shown here for conciseness.

The Magnitude-Squared Coherence (MSC) between the time signals acquired in the far-field and on the airfoil surface tappings is shown in Fig. 12 for the hard wall and over-tip liner configurations ( $h = 20$  mm).

The coherence between the wall pressure at the airfoil tip location at 50% of the chord and the pressure side far-field microphone ( $\theta = -90^\circ$ ) is shown in Fig. 12(a). The reduction in the wall pressure fluctuations at  $x/c = 0.5$  due to the liner previously observed in Fig. 10(b) corresponds to a drastic reduction in coherence over the higher frequencies ③. This result suggests that the liner significantly suppresses sources of noise radiating from the mid-chord region over this frequency range. The coherence of the lined and hard wall cases is, however, practically identical at the anti-resonance frequency of the liner ( $f \approx 8.5$  kHz) as expected from acoustic back-reactions. However, the values of coherence at those high frequencies are small even in the hard wall case due to the distributed nature of the tip leakage noise in ③. A loss of coherence is also observed at the frequencies of the first hump ①, although this is most evident in the coherence between the wall pressures in  $x/c = 0.75$  and the far-field microphone ( $\theta = -90^\circ$ ) shown in Fig. 12(b). The hard wall data in Fig. 12(b) clearly indicate the role of the unsteady pressures in this area of the airfoil tip to the far-field noise over the frequencies of the first hump ① due to the high values of coherence up to almost  $MSC = 0.5$ . The coherence is, however, significantly reduced with the liner, as well as the magnitude of the wall pressures previously shown in Fig. 10(d). Once again, the reduction in the magnitude of coherence and the slight increase in the peak frequency in Fig. 10(d) when the liner is present suggests that the tip flow separation has moved further downstream of the chord. This is consistent with recent work that investigated the sensitivity of the tip leakage noise with the angle of attack and the location of the separated flow.<sup>22</sup>

Note that MSC results are shown for the cavity depth  $h = 20$  mm since synchronous far-field and surface pressure measurements were only obtained for this configuration, alongside the flow measurements presented in Sec. IV C. It has been shown earlier, however, that the liners present the same qualitative behavior with all cavity depths and just yield the peak noise reductions and the anti-resonances at different frequencies.

The results in this section confirm that over-tip liners modify the unsteady pressure fluctuations on the airfoil tip at key locations relevant to the generation of tip-leakage noise. In addition, the results in Fig. 12 indicate that over-tip liners can significantly suppress tip-leakage noise by acting on the airfoil tip region. It has been argued that these source modifications are dominated by *acoustic* back-reaction effects for the smaller gaps of  $e = 5$  mm, in which tip noise is distributed incoherently along the chord at the tip edge. It has been shown that in such circumstances, the source modifications can be predicted with simplified analytical models and tuned by liner design parameters (in this case the cavity depth). It has been hypothesized, however, that the noise suppression at the larger tip gap of  $e = 10$  mm is no longer dominated by acoustic back-reaction on the source over frequencies of the first and second humps ① and ②. In this case, the large coherent structures in the tip-leakage flow field responsible for the generation of noise in ① and ② can also be weakened by the presence of the liner and the location of the separated flow region can be moved, causing large reductions in the wall pressures fluctuations on the airfoil tip. The effect of the liners on the tip leakage flow is investigated in Sec. IV C.

#### On the near-to-far field causality measurements

The far-field noise due to boundary layer-induced wall-pressure fluctuations near an airfoil trailing edge can be predicted by using Amiet's theory.<sup>27</sup> However, multiple mechanisms other than trailing edge noise have been proposed in the literature for the more complex 3D problem of tip-leakage noise. A modified version of Amiet's theory with spanwise attenuation to damp the perturbations away from the tip was proposed in the literature<sup>25</sup> to model the tip gap noise generated by the turbulent eddies in the cross-flow as they are scattered by the tip suction side edge. The role of the lower plate corresponding to the casing in a ducted fan was assumed to be equivalent to introducing the image of the airfoil with respect to the lower plate. This assumption is not valid, however, for the case of over-tip liners, in which a non-rigid boundary condition is imposed in the near-field of the tip leakage sources. The simplistic approach taken in this section based on a direct comparison of the reductions in wall pressures and far-field noise, and the coherence between the signals, does not account for scattering nor masking effects by the airfoil. However, it provides a first indication of the effect of over-tip liners in the absence of established analytical models of tip-leakage noise with non-rigid boundary conditions.

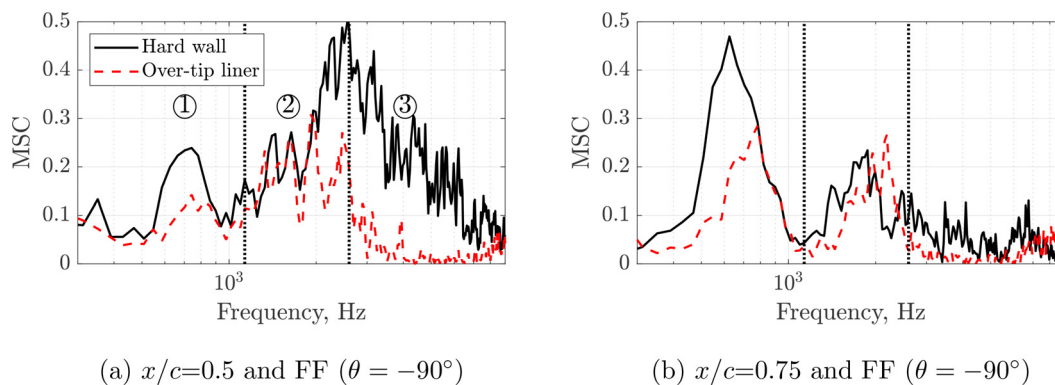


FIG. 12. MSC between wall pressure fluctuations at the tip and far-field noise for the hard wall baseline and the over-tip liner ( $h = 20$  cm) for  $e = 10$  mm.



C. Effect of the over-tip liners on the tip leakage flow

This section focuses on evaluating the effect of the over-tip liner on the flow field in the tip region. Synchronous measurements of the unsteady velocities close to the tip, airfoil tip wall pressures, and far-field pressures were performed for the hard wall and the over-tip liner configurations. The steady pressures at the pressure tapings located at 1 mm from the airfoil tip were also measured for both the hard and lined cases. The results are shown for the over-tip liner configuration with  $h = 20$  mm.

The steady pressures for the hard and lined cases are compared in Fig. 13 for the two tip gap sizes  $e = 5$  and 10 mm in the form of pressure coefficients, defined as  $C_p = \frac{p - p_\infty}{\frac{1}{2}\rho_\infty U_\infty^2}$ , where  $p_\infty$  is the reference pressure measured in zero flow conditions,  $\rho_\infty = 1.225 \text{ kg/m}^3$  is the mean flow density, and  $U_\infty = 40 \text{ m/s}$  the mean flow velocity.

The comparison in Fig. 13 indicates that the over-tip liner has a limited effect in changing the mean pressure distribution on the airfoil tip. This was expected since the smooth wire mesh used for the liner designs is known to have minimal impact on the grazing flow over the liner surface, especially in comparison to liners with a perforated facing sheet. However, for the case of  $e = 10$  mm, the small change in pressure gradient on the suction side of the airfoil around the mid-chord position can indicate a modification of the flow separation in the tip region.<sup>22</sup> This is investigated next based on the hot-wire flow measurements.

The normalized mean velocity measured with the hot-wire in the locations shown in Fig. 5(a) (red dots) is shown in Fig. 14 for the hard wall and over-tip liner configurations. The position of the airfoil tip is indicated with a horizontal black line, and the axis is normalized with the airfoil chord. The mean velocity maps are characterized by two common elements. The first is the area of low velocity starting from around 33% attributed to flow separated from the pressure side tip edge. The second is the cross-flow through the gap and close to the wall surface, which is strongest between roughly 50% and 75% of the chord. These elements are consistent with previous experimental<sup>10</sup> and computational<sup>17</sup> work and the recent analysis by the authors on the noise generation mechanisms in the current setup.<sup>20,22</sup> A comparison of Figs. 14(a) and 14(b) clearly shows that the over-tip liner affects the mean flow close to the liner surface ( $z/c = 0$ ) by reducing the magnitude of the cross-flow, from a maximum velocity of  $\sqrt{V^2 + W^2}/U_0 \approx 1$  in the hard wall configuration down to

$\sqrt{V^2 + W^2}/U_0 \approx 0.75$  when the liner is present. There is therefore a loss of momentum close to the liner surface and a weaker shear layer.

The results in Fig. 14 do not give information about the frequency content of the near-wall flow field and cannot be directly used to understand the effect of the loss of momentum on the noise signature measured by wall pressure probes and far-field microphones. The velocity auto-spectrum at different heights of the hot-wire probe from the wall is therefore shown in Fig. 15 for a selection of locations in the  $x$ - $y$  plane [indicated in Fig. 15(a)]. These are listed below.

- $x/c = 0.37$ : The tip cross-flow in this location is very weak. Comparison of Figs. 15(b) and 15(c) indicates that the over-tip liner has a negligible effect on the flow in this region of the airfoil tip. This location is shown as a reference of what would be expected in the case of conventional grazing flow over an SDOF liner with a wire mesh.
- $x/c = 0.50$ : This location corresponds to the start of the cross-flow region. A strong broadband component is observed centered at  $z = 6$  mm, indicating the shear layer and the separated flow region. The liner is found in this instance to slightly increase the velocity fluctuations very close to the wall [Figs. 15(d) and 15(e)] at frequencies above 1 kHz.
- $x/c = 0.74$ : Large coherent structures caused by vortex shedding have been shown to induce unsteady forces on the airfoil responsible for the dominant source at low frequencies ①, characterized by a hump around 800 Hz.<sup>20</sup> These are strongest in the region around 75% of the chord. In addition, smaller scale flow structures attributed to the noise for the second hump ② ( $1100 < f < 2600 \text{ Hz}$ ). The unsteady velocities are indeed found to be more significant around 800 Hz and  $1100 < f < 2600 \text{ Hz}$  in the hard wall case [Fig. 15(f)], but these are practically suppressed when the over-tip liner is installed [Fig. 15(g)]. This can be both due to the weakening of the shear layer and to the movement of the separated flow toward more downstream locations.

The results in Figs. 15(f) and 15(g) indicate that the over-tip liner has dramatic effects in mitigating the strong unsteady flow features responsible for the noise over both the first and second humps ① and ② at  $e = 10$  mm. The liner is therefore not only suppressing noise by acoustic attenuation and back-reaction effects on the source but also by modifying the tip leakage flow. This result is in agreement with the

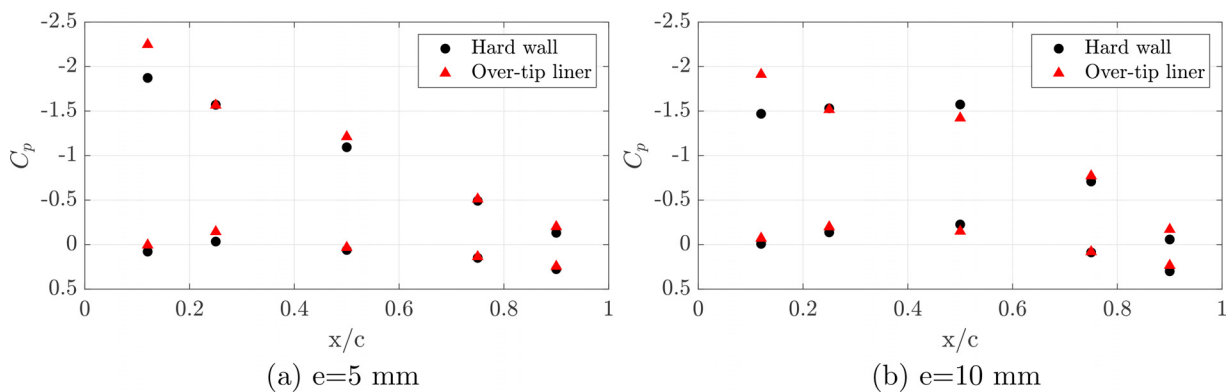


FIG. 13. Comparison of the pressure coefficient ( $C_p$ ) measured at 1 mm from the tip edge for the hard wall and over-tip liner configurations.

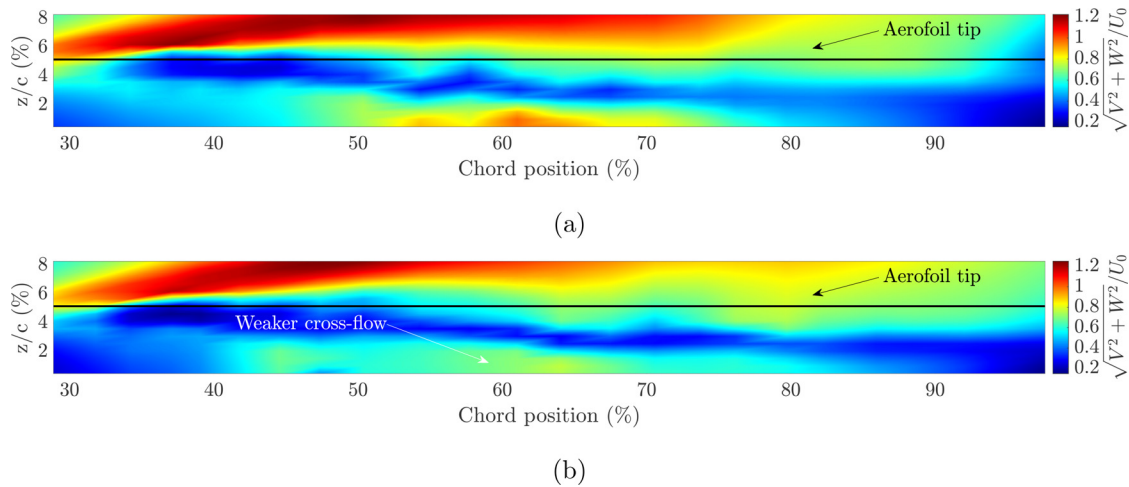


FIG. 14. Normalized mean velocity field in the hot-wire plane for (a) the hard wall and (b) over-tip liner.

finding from Fig. 9 that the over-tip liners tested in this investigation yield insertion loss in the far-field over frequencies of the first hump ① regardless of the cavity depth  $h$ , even when the analytical predictions indicate they should not produce any noise reductions at those frequencies [Fig. 9(b)].

To further support the finding above, a conditional averaging technique is used to identify the flow structures involved in the noise generation over ① and ② for the hard wall and lined configurations.<sup>20,22</sup> Hot-wire velocity data for  $e = 10$  mm measured in a plane-parallel to the bottom plate and at a height of  $z = 5$  mm from it [Fig. 5(a), blue dots] are used in this analysis. The velocity data are correlated with the far-field pressure signals and bandpass filtered in the frequency range of the first and the second humps, ① and ②, respectively. This covariance  $Cov_{u-p}$  between the velocity and the pressure signals is evaluated by using

$$Cov_{u-p} = \frac{1}{N-1} \sum_{n=1}^N u \times p(\tau), \quad (12)$$

where  $\tau$  is the time delay between the far-field microphone and the hot wire probe,  $u$  and  $p$  are the velocity and pressure fluctuations, respectively, and  $N$  is the number of samples. The resulting covariance for the hard wall and lined configurations is shown in Fig. 16.

The flow structures responsible for the tip noise for the hard wall case at the frequencies of the first and second humps can be observed in Figs. 16(a) and 16(c), respectively. The detailed analysis of the noise generation mechanisms for the hard wall baseline is not the subject of this investigation and can be found in the literature.<sup>22</sup> However, the over-tip liner has a dramatic impact on these flow structures. The patterns in the covariance plots when the liner are present are less clear both for the frequencies of the first hump ① [Fig. 16(b)] and the second hump ② [Fig. 16(d)], and the levels are drastically reduced, as shown by the limits of the colourmap.

The covariance results in Fig. 16 further support the hypothesis that the over-tip liner modifies the unsteady flow features in the gap region responsible for the generation of noise over frequencies ① and

② for  $e = 10$  mm. The mechanism by which the over-tip liners modify the tip leakage flow is investigated next.

Acoustic liners with a smooth wire mesh conventionally installed in the intake or bypass regions of aero engines are generally regarded as causing very little impact on the mean flow characteristics. The liners operate under grazing flow conditions in those instances. However, in the case of over-tip liners, the three-dimensional tip leakage flow could result in flow penetration in cavity cells below the tip region. This hypothesis is investigated by measuring the flow within the liner cavity cells immediately below the airfoil tip pressure side edge. A hot wire probe was located at the center of the honeycomb cell at various depths  $d = 5$ –15 mm from the wire mesh plane as shown in Fig. 5(b). These measurements were performed for a conventional grazing flow condition (without the airfoil) and for the tip leakage flow configuration.

The measured velocities within the cavities are shown in Fig. 17 for the two tip gaps  $e = 5$  and 10 mm at two cells located below the pressure side edge at  $x/c = 0.5$  and  $x/c = 0.75$ , where  $d = 0$  mm corresponds to the location of the wire mesh and  $d = -20$  mm the location at the bottom of the cavity cell (backing sheet). The measured velocity in the plane normal to the single wire is simplified here as  $v^*$ . The flow within the cavities is negligible for the grazing conditions. Conversely, in the cases with tip leakage flow, non-zero velocities are measured within the liner cavities, which can be stronger close to the wire mesh ( $d = -5$  mm) for the lower gap size of  $e = 5$  mm. Variations in magnitude at different depths  $d$  are expected due to flow recirculation within the cavities. An analysis of the flow within the cavities is, however, outside the scope of this study, and hot-wire measurement is not the most appropriate technique to characterize the very low flow velocities within the cavities. However, these results show experimentally for the first time that over-tip liners are likely to experience bias flow and that, in turn, can cause modifications in the flow features in the tip area responsible for the generation of tip leakage noise.

It is hypothesized that the dissipation of kinetic energy in the facing sheet caused by the flow penetration into the liner cells can be responsible for the loss of momentum in the cross-flow observed in Fig. 14. The reduced cross-flow would also lead to a weaker shear layer

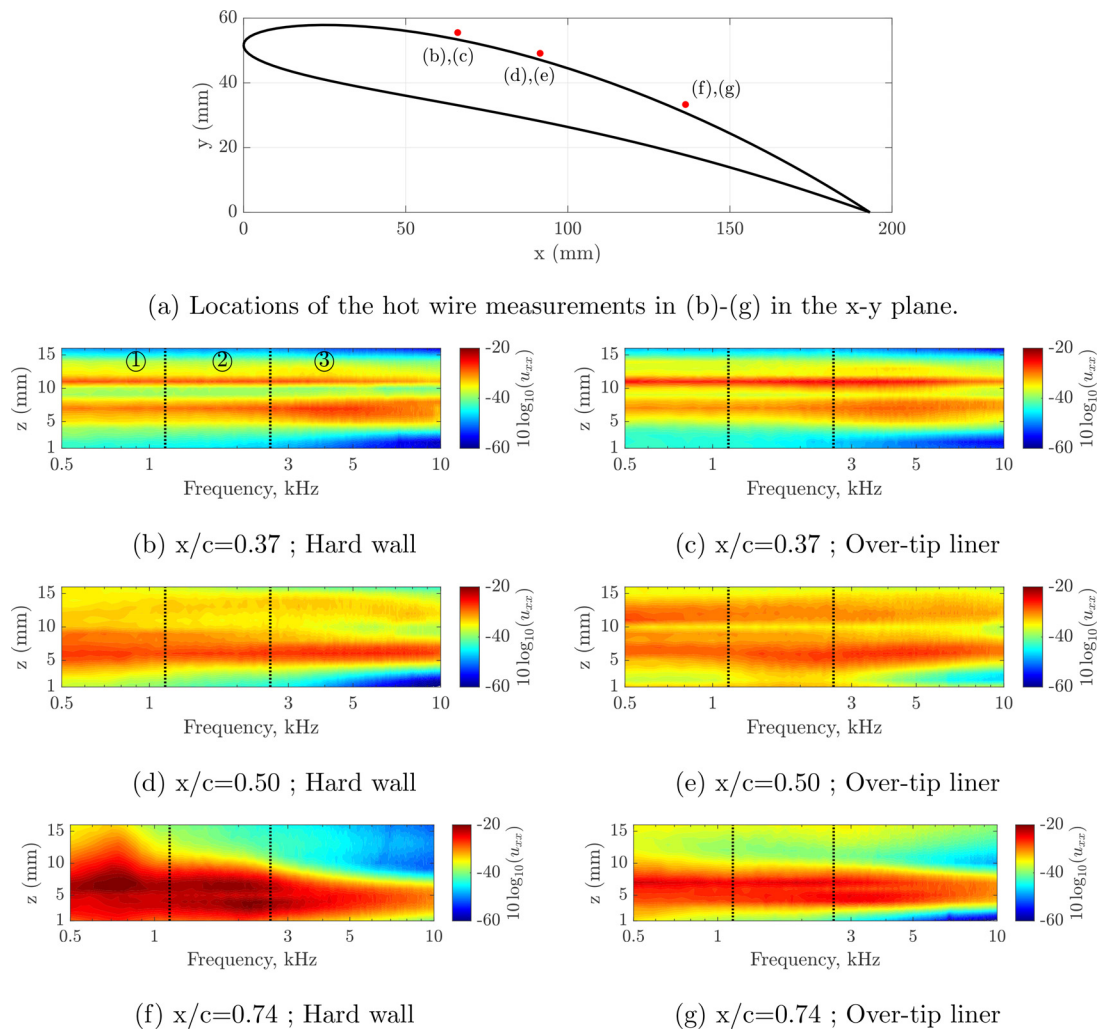


**FIG. 15.** Comparison of the velocity spectra in the tip region for a hard wall and over-tip liner at different heights from the wall ( $z$ ) and measurement locations ( $x/c$ ) for  $e = 10$  mm.

and vortex shedding and hence the mitigation of the flow structures responsible for the generation of noise over frequencies ① and ② at  $e = 10$  mm. A similar effect has also been reported when a thicker boundary layer is present.<sup>22</sup>

### V. CONCLUSIONS

This paper has experimentally investigated the reductions of tip-leakage noise by using over-tip liners. The Over-Tip-Rotor liner configuration has been approximated by an instrumented static airfoil with its tip located over a flat plate containing a flush-mounted liner insert and separated from the airfoil tip by a small gap. The results of synchronous measurements of the unsteady velocities close to the tip, the wall pressures on the airfoil tip, and far-field pressures have been presented for the hard wall and the over-tip liner configurations.

It has been experimentally confirmed for the first time in the literature that over-tip liners modify the unsteady wall pressure on the airfoil tip at locations relevant to the generation of tip-leakage noise.

These reductions in wall pressure at the tip are found to correspond to frequencies of peak far-field noise reductions, over which the coherence between the wall pressures and far-field noise is drastically reduced when an over-tip liner is installed.

Over-tip liners are found to modify the sources of high-frequency tip leakage noise mainly through *acoustic* back-reaction effects on the source, which can be tuned with the design of the liners. The good qualitative agreement with simple analytical models suggests that they can be used to provide guidance in the design of OTR liners for optimum noise reduction and tune them at target frequencies of interest.

It has also been experimentally shown for the first time that over-tip liners can modify the tip-leakage flow. The liners weaken the coherent flow structures in the tip area responsible for the generation of tip leakage noise at low- to mid-frequencies (for  $e = 10$  mm), therefore causing a *hydrodynamic* source modification. Flow measurements within the liner cavities below the airfoil tip have experimentally

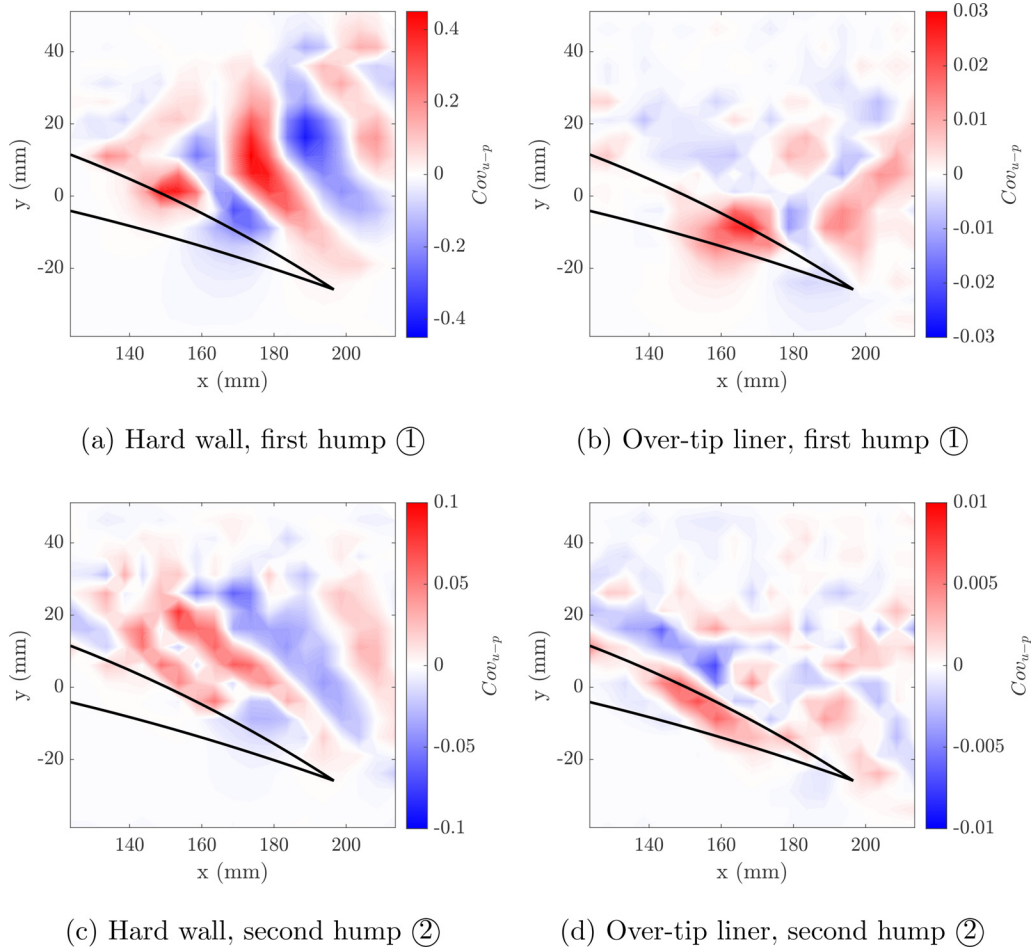


FIG. 16. Covariance  $Cov_{u-p}$  obtained correlating the velocity fluctuations and the pressure measurements filtered in the frequency range first and second humps ① and ② for  $e = 10$  mm.

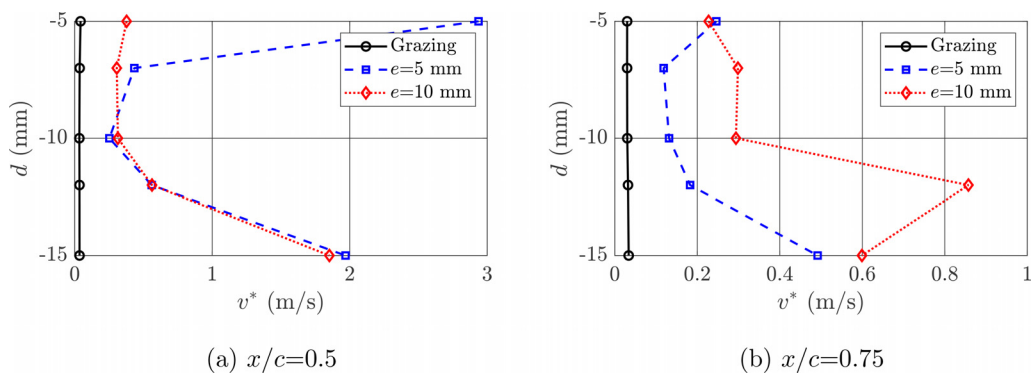


FIG. 17. Mean velocity measured within the over-tip liner cavities located immediately below the airfoil pressure side edge for grazing flow and tip-leakage flow conditions.

confirmed that over-tip liners can experience bias flow. This can be a possible cause for the modifications in the tip leakage flow structures through dissipation of kinetic energy at the facing sheet and loss of momentum in the tip cross-flow.

This investigation has shed new light on the so-called source modification effects of over-tip rotor liners and confirmed that these are both caused by *acoustic* back-reaction effects and *hydrodynamic* modifications of the source. An explicit formulation has also been



presented to link these effects to the physics of the generation of noise at the airfoil tip. However, further studies would be beneficial to confirm the mechanism by which the liner bias flow modifies the tip leakage flow features and the sources of tip leakage noise. Numerical simulations that include the airfoil blade and the liner could be particularly useful for this purpose but are outside the scope of the current investigation.

## ACKNOWLEDGMENTS

This work was funded by the Royal Academy of Engineering (RF\201819\18\194) and by the Engineering and Physical Sciences Research Council (EP/V00686X/1). The authors would like to thank Professor Phil Joseph for his insight on the acoustic power of tip-leakage noise presented in Sec. III B. The authors would also like to thank Dr. Paul Murray for measuring the liner impedance, Dr. Suresh Palani for valuable discussions, and Rolls-Royce for technical support.

## AUTHOR DECLARATIONS

### Conflict of Interest

The authors have no conflicts to disclose.

## Author Contributions

**Sergi Palleja-Cabre:** Conceptualization (equal); Data curation (lead); Formal analysis (lead); Investigation (equal); Methodology (equal); Validation (lead); Writing – original draft (lead); Writing – review & editing (lead). **Ivan Saraceno:** Data curation (equal); Formal analysis (equal); Investigation (equal); Methodology (equal); Writing – review & editing (equal). **Paruchuri Chaitanya:** Conceptualization (equal); Funding acquisition (lead); Investigation (equal); Methodology (equal); Writing – review & editing (equal).

## DATA AVAILABILITY

The data that support the findings of this study are available from the corresponding author upon reasonable request.

## REFERENCES

- S. Moreau, “Turbomachinery noise predictions: Present and future,” *Acoustics* **1**, 92–116 (2019).
- D. L. Sutliff, M. G. Jones, and T. C. Hartley, “High-speed turbofan noise reduction using foam-metal liner over-the-rotor,” *J. Aircr.* **50**, 1491–1503 (2013).
- M. R. Gazella, T. Takakura, D. L. Sutliff, R. Bozak, and B. J. Tester, “Evaluating the acoustic benefits of over-the-rotor acoustic treatments installed on the advanced noise control fan,” AIAA Paper No. 2017-3872, 2017.
- R. Bozak and R. P. Dougherty, “Measurement of noise reduction from acoustic casing treatments installed over a subscale high bypass ratio turbofan rotor,” AIAA Paper No. 2018-4099, 2018.
- D. L. Sutliff, R. F. Bozak, M. G. Jones, and D. M. Nark, “Investigations of three over-the-rotor liner concepts at various technology readiness levels,” *Int. J. Aeroacoust.* **20**, 826–866 (2021).
- S. Palleja-Cabre, B. J. Tester, and R. J. Astley, “Modelling of ducted noise sources in the proximity of acoustic liners,” *J. Sound Vib.* **517**, 116548 (2021).
- S. Palleja-Cabre, B. J. Tester, and R. J. Astley, “Modeling of over-tip-rotor liners for the suppression of fan noise,” *AIAA J.* **60**, 6361–6373 (2022).
- S. Palleja-Cabre, B. J. Tester, R. J. Astley, and G. Bampanis, “Aeroacoustic assessment of performance of overtip liners in reducing airfoil noise,” *AIAA J.* **59**, 3622–3637 (2021).
- J. Grilliat, M. Jacob, R. Camussi, and G. Caputi-Gennaro, “Tip leakage experiment - Part one: Aerodynamic and acoustic measurements,” AIAA Paper No. 2007-3684, 2007.
- M. C. Jacob, J. Grilliat, R. Camussi, and G. C. Gennaro, “Aeroacoustic investigation of a single airfoil tip leakage flow,” *Int. J. Aeroacoust.* **9**, 253–272 (2010).
- S. Thomasson, “Reflection of waves from a point source by an impedance boundary,” *J. Acoust. Soc. Am.* **59**, 780 (1976).
- Y. Sun, X. Wang, L. Du, and X. Sun, “On the flow-acoustic coupling of fan blades with over-the-rotor liner,” *J. Fluid Mech.* **941**, A67 (2022).
- S. Palleja-Cabre, I. Saraceno, S. Palani, and P. Chaitanya, “Reduction of tip-leakage noise by using over-tip liners,” *AIAA Paper No. 2022-2930*, 2022.
- R. R. Subramanyam, S. Palani, P. Chaitanya, and S. Palleja-Cabre, “On the noise reduction mechanism of over-tip liners,” *J. Acoust. Soc. Am.* **155**, 29–43 (2024).
- P. Zhao, Z. Zhao, and C. Yang, “Investigation of the orifice flow of over-the-rotor liner and its interaction with the rotor flow field,” *Phys. Fluids* **35**, 107144 (2023).
- T. P. Chong, P. F. Joseph, and P. O. A. L. Davies, “A parametric study of passive flow control for a short, high area ratio 90 deg curved diffuser,” *J. Fluids Eng.* **130**(11), 111104 (2008).
- R. Koch, M. Sanjosé, and S. Moreau, “Large-eddy simulation of a single airfoil tip-leakage flow,” *AIAA J.* **59**, 2546–2557 (2021).
- Brüel & Kjaer, Sound & Vibration, Product Information Portable Impedance Meter System – Type 9737, 2014.
- R. E. Mottsigner and R. K. Kraft, “Design and performance of duct acoustic treatment,” in *Aeroacoustics of Flight Vehicles: Theory and Practice. Volume 2: Noise Control* (NASA, Washington, D.C. 1991).
- I. Saraceno, S. Palleja-cabre, P. Chaitanya, P. Jaiswal, and B. Ganapathisubramani, “On the tip leakage noise generating mechanism of single-fixed aerofoil,” AIAA Paper No. 2022-2881, 2022.
- H. Levine, “Output of acoustical sources,” *J. Acoust. Soc. Am.* **67**(6), 1935–1946 (1980).
- I. Saraceno, S. Palleja Cabre, P. Chaitanya, and B. Ganapathisubramani, “Influence of non-dimensional parameters on the tip leakage noise,” AIAA Paper No. 2023-3838, 2023.
- H. Levine, “On source radiation,” *J. Acoust. Soc. Am.* **68**, 1199–1205 (1980).
- P. A. Nelson and S. J. Elliott, “Active minimisation of acoustic fields,” *J. Theor. Appl. Mech.* **6**, 39–89 (1987).
- J. Grilliat, E. Jondeau, M. C. Jacob, M. Roger, and R. Camussi, “Broadband noise prediction models and measurements of tip leakage flows,” AIAA Paper No. 2008-2845, 2008.
- R. Camussi, J. Grilliat, G. Caputi-Gennaro, and M. C. Jacob, “Experimental study of a tip leakage flow: Wavelet analysis of pressure fluctuations,” *J. Fluid Mech.* **660**, 87–113 (2010).
- R. K. Amiet, “Noise due to turbulent flow past a trailing edge,” *J. Sound Vib.* **47**, 387–393 (1976).